
Extrapolation Methods and Scaled Perturbation Theory for Determining Intermolecular Potential Energy Surfaces

MATTHEW P. HODGES, ELENA BICHOUTSKAIA,
AKYL S. TULEGENOV, RICHARD J. WHEATLEY

*School of Chemistry, University of Nottingham, University Park, Nottingham, NG7 2RD,
United Kingdom*

Received 6 September 2002; accepted 28 May 2003

DOI 10.1002/qua.10747

ABSTRACT: We construct potential energy curves for six rare-gas dimers and several 1-D cuts through two $\text{H}_2 \cdots$ rare-gas potential energy surfaces using two methods. The first is based on supermolecule dimer calculations at a low level of theory, extrapolated using monomer calculations at higher levels of theory. The second is based on perturbation theory calculations, where the effects of intramolecular electron correlation on different interaction terms are treated using approximate scaling relationships. Both methods are competitive with supermolecule dimer calculations at higher levels of theory and provide computationally efficient means of studying weakly bound systems. The methods are therefore suitable for calculations on larger systems for which accurate supermolecule methods would be computationally expensive.

© 2003 Wiley Periodicals, Inc. *Int J Quantum Chem* 96: 537–546, 2004

Key words: extrapolation; intermolecular forces; molecular hydrogen; perturbation theory; rare gases

1. Introduction

The class of chemical systems bound by weak van der Waals forces or hydrogen bonds provides particular challenges to theoretical chemists.

Correspondence to: M. P. Hodges; e-mail: matt@tc.bham.ac.uk
M. P. Hodges' present address is School of Chemistry, The University of Birmingham, Edgbaston, Birmingham, B15 2TT, United Kingdom.

Wide areas of research involving noncovalent interactions depend on a description of the potential energy surface, whether this be aiding the interpretation of high-resolution spectroscopic data or modeling the binding of ligands to proteins. Whatever the application, the accuracy of the potential energy surface used in any calculation is a factor that must be considered when interpreting results, and there is no doubt that only for a small number of systems are accurate intermolecular potentials available.

The target of “chemical accuracy,” often quoted as 1 kcal/mol, may be a significant fraction of the binding energy for hydrogen-bonded systems such as the water dimer, or indeed many times the binding energy for van der Waals systems bound primarily by dispersion forces. On the other hand, “spectroscopic accuracy” (i.e., 1 cm⁻¹) is much more appropriate for weakly bound systems, 1 cm⁻¹ being about 1% of the argon dimer binding energy, but still representing over 10% of the helium dimer interaction. Accuracy of 1% in the binding energy of a van der Waal complex is still not, in general, an easy target to achieve, principally due to present computational limitations. Post-Hartree–Fock supermolecule methods using large basis sets lead to calculations that scale unfavorably with system size, and the number of systems for which essentially exact solutions of the nonrelativistic Schrödinger equation (within the Born–Oppenheimer approximation) can be obtained is limited to those with a small number of electronic degrees of freedom.

In this article we test two methods for obtaining potential energy surfaces for weakly bound systems at reduced computational cost relative to supermolecule dimer calculations at high levels of theory. The principal means of achieving this is by partitioning interaction energies into physically meaningful pieces and avoiding the explicit calculation of contributions that we can model in more computationally efficient ways. We test our methods on the three homonuclear and three heteronuclear rare-gas dimers containing helium, neon, and argon, and also show preliminary results for the H₂ ··· Ne and H₂ ··· Ar systems. The rare-gas dimer potential energy curves have been extensively researched over the last 30 years (see, e.g., the extensive review of Aziz [1], documenting the common methodologies used), and accurate semiempirical Hartree–Fock plus dispersion (HFD) potentials are available. Extensive ab initio studies of both homo- and heteronuclear systems have also recently been carried out [2]. Several theoretical and spectroscopic determinations of the H₂ ··· Ne and H₂ ··· Ar potential energy surfaces have also been made.

2. Methods

We now describe the two methods we use to calculate interatomic and intermolecular potential energy curves. The first, the Systematic InterMo-

lecular Potential Extrapolation Routine (SIMPER), was first described in a previous article [3], where a procedure to estimate high-level dimer energies using low-level dimer energies and high-level monomer properties was outlined. Refinement of the SIMPER method is described in Section 2.1. The second method, scaled perturbation theory (SPT), is based on calculation of low-order terms arising from the interaction Hamiltonian; this is described in Section 2.2.

Both approaches use an extension to the overlap model (see, e.g., Ref. [4]) that we developed [5] to estimate the effects of electron correlation on exchange contributions. We showed that first-order exchange energies at the MP2 level could be approximated using first-order self-consistent field (SCF) exchange energies and SCF and MP2 charge-density overlap integrals:

$$E_{\text{exch}}^{\text{MP2}} \approx E_{\text{exch}}^{\text{SCF}} \times \frac{S_p^{\text{MP2}}}{S_p^{\text{SCF}}} \quad (1)$$

Because the ratio of the exchange energy and the charge density overlap integral is not strongly dependent on the level of theory, Eq. (1) can be generalized to apply to any two levels of theory,

$$E_{\text{exch}}^{\text{level 2}} \approx E_{\text{exch}}^{\text{level 1}} \times \frac{S_p^{\text{level 2}}}{S_p^{\text{level 1}}}, \quad (2)$$

and we have shown this to be accurate for the helium dimer with full configuration interaction (FCI) as “level 2” and SCF as “level 1” [6]. The levels of theory at which we calculate charge density overlap integrals in this work are SCF, second-order Møller–Plesset perturbation theory (MP2), and quadratic configuration interaction with single and double substitutions (QCISD). The atomic and molecular charge densities are calculated using Molpro [7], and first-order Coulomb energies are also calculated directly from these.

We also calculate, again using Molpro, ab initio interaction energies at the MP2 and coupled-cluster with single, double, and perturbative triple substitutions [CCSD(T)] levels of theory. The neon 1s and argon 1s, 2s, and 2p core orbitals are frozen, and we use the full counterpoise procedure of Boys and Bernardi [8] in all cases. The aug-cc-pV5Z basis sets of Dunning and coworkers [9, 10], and modified versions of these are used, where the latter have the exponents of the polarization functions shifted using a simple scheme, principally to improve the

dispersion interaction [6, 11]. Henceforth, we refer to the standard and “shifted polarization” 5- ζ basis sets as AV5Z and SP-AV5Z.

2.1. SIMPER METHOD

The intermolecular potential energy extrapolation method can be described as follows. We divide the MP2 interaction energy into exchange, first-order Coulomb, second-order dispersion, and all other Coulomb contributions:

$$\Delta E_{\text{int}}(\text{MP2}) = E_{\text{exch}} + E_{\text{Coul}}^{(1)} + E_{\text{disp}}^{(20)} + E_{\text{Coul}}^{\text{rest}} \quad (3)$$

The first-order Coulomb interaction energy is calculated from the unperturbed ground-state charge densities. We replace the first-order Coulomb energy at the MP2 level by the first-order QCISD Coulomb energy. For rare-gas dimers, the induction component of the interaction energy is relatively small, has no long-range multipolar component, and we do not extrapolate it; this is combined with higher-order terms in $E_{\text{Coul}}^{\text{rest}}$.

The dispersion and exchange energies are much more important and require extrapolation to a higher level of theory for accurate work. We calculate dispersion energy coefficients, C_N^{MP2} , corresponding to the asymptotic behavior of $E_{\text{disp}}^{(20)}$ at long range, and represent the dispersion energy by a damped multipolar series:

$$E_{\text{disp}}^{(20)} = - \sum_N C_N^{\text{MP2}} \cdot f_N(b^{\text{MP2}}R) \cdot R^{-N}, \quad (4)$$

where the $f_N(bR)$ are Tang–Toennies damping functions [12] (i.e., incomplete gamma functions of order $N + 1$), and the scaling parameter b^{MP2} is obtained at each point on the potential energy surface because all the other quantities are known.

The MP2 damping functions can be improved by assuming that the scale parameters, b , are proportional to $(C_6/C_8)^{1/2}$ [13] such that

$$b^{\text{CISD}} \times \sqrt{\frac{C_8^{\text{CISD}}}{C_6^{\text{CISD}}}} \approx b^{\text{MP2}} \times \sqrt{\frac{C_8^{\text{MP2}}}{C_6^{\text{MP2}}}} \quad (5)$$

The extrapolated dispersion energy is obtained by substituting more accurate TD-CISD dispersion energy coefficients (calculated separately) and scaling parameters [obtained from Eq. (5) at each point on the potential energy surface] for the MP2 values in

Eq. (4). Importantly, no fitting is involved in the extrapolation procedure for the dispersion energy.

Extrapolation of the dominant short-range component of the interaction, the exchange energy, is done using Eq. (2). Note that in the original formulation of this method only the first-order exchange was treated, but we do not partition the exchange into first- and higher-order contributions using SIMPER so all orders of exchange are scaled using the ratio of QCISD and MP2 charge density overlap integrals. Again, no fitting procedure is required.

The extrapolated (SIMPER) interaction energy is hence the sum of the extrapolated exchange energy, the directly calculated first-order QCISD Coulomb energy, the extrapolated second-order dispersion energy, plus the unscaled MP2 induction energy and miscellaneous higher-order terms. This improves on the description of the dispersion energy presented in the original SIMPER work [3], which was believed to be the main deficiency in the method.

2.2. SPT METHOD

The SPT method is more established than the newer SIMPER approach, and we have developed a number of SPT intermolecular potentials ($\text{NH}_3 \cdots \text{He}$ [14], $\text{H}_2\text{O} \cdots \text{He}$ [15], $\text{H}_2\text{O} \cdots \text{Ne/Ar}$ [11], and $\text{He} \cdots \text{He}$ [6]). This method has been refined over the last few years to approach a consistent and accurate framework with which all weakly bound systems can be treated. We describe here the current SPT methodology that we apply to all systems considered in this work.

The first-order exchange, $E_{\text{exch}}^{(10)}$, is calculated using the Heitler–London (HL) method and scaled according to Eq. (2), using the ratio of QCISD and SCF charge density overlap integrals. First-order Coulomb energies are calculated directly using the QCISD charge densities.

Second-order coupled Hartree–Fock (CHF) induction energies, $E_{\text{ind}}^{\text{CHF}}$, and time-dependent coupled Hartree–Fock (TDCHF) dispersion energies are calculated using the random-phase approximation (RPA) spectrum of excited states. The dispersion energies are scaled isotropically by $C_6^{\text{DOSD}}/C_6^{\text{RPA}}$, i.e., the ratio of constrained dipole oscillator strength distribution (DOSD) [16, 17] and our RPA values of the leading dispersion energy coefficient, C_6 . This guarantees the correct long-range (R^{-6}) behavior for each system. To estimate the effects of intramolecular electron correlation on the induction energies, the CHF components are scaled by the

ratio of induction contributions calculated at the MP2 and SCF levels of theory, in the SCF field of the second monomer, i.e., the contribution for fragment A we use is:

$$E_{\text{ind}}^{\text{MP2}}(A) \approx E_{\text{ind}}^{\text{CHF}}(A) \times \frac{E_{\text{ind}}^{\text{ff,MP2}}(A[B])}{E_{\text{ind}}^{\text{ff,SCF}}(A[B])}, \quad (6)$$

where “ff” indicates a finite-field calculation, in this case for fragment A in the environment of B (here signified using the notation $A[B]$). For systems with multipolar contributions, an alternative to using Eq. (6) is to multiply each fragment contribution by the ratio of the fragment’s MP2 and SCF dipole polarizabilities; preliminary work on $\text{H}_2\text{O} \cdots \text{H}_2$ indicates that this computationally simpler method yields similar results to the finite-field calculations, although at a reduced computational cost.

Higher-order exchange terms are included as follows. The exchange induction contribution is estimated from supermolecule SCF interaction energies by assuming the following decomposition:

$$\Delta E_{\text{int}}(\text{SCF}) \approx \Delta E_{\text{HL}} + E_{\text{ind}}^{\text{CHF}} + E_{\text{exch-ind}}(\text{SCF}), \quad (7)$$

where we neglect charge transfer and higher-order induction effects, which are expected to be small in these nonpolar systems. A similar approach is used to estimate the exchange dispersion contribution. In this case, MP2 supermolecule interaction energies are decomposed according to

$$\Delta E_{\text{int}}(\text{MP2}) \approx E_{\text{exch}}^{(1)} + E_{\text{Coul}}^{(1)} + E_{\text{ind}} + E_{\text{disp}}^{(20)} + E_{\text{exch-ind}} + E_{\text{exch-disp}}, \quad (8)$$

where the exchange contribution is calculated using Eq. (2), the first-order Coulomb contribution directly using the MP2 charge densities, the induction contribution using the sum of A and B components from Eq. (6), and the dispersion contribution at the uncoupled Hartree–Fock (UCHF) level of theory. The exchange induction used here is that calculated by Eq. (7) and scaled by the ratio of the MP2 and SCF overlap integrals. The final SPT interaction energies are the sum of the first-order exchange and Coulomb contributions at the QCISD monomer level of theory, induction and second-order exchange at approximately the MP2 level of theory, and dispersion isotropically scaled to reproduce the correct long-range behavior.

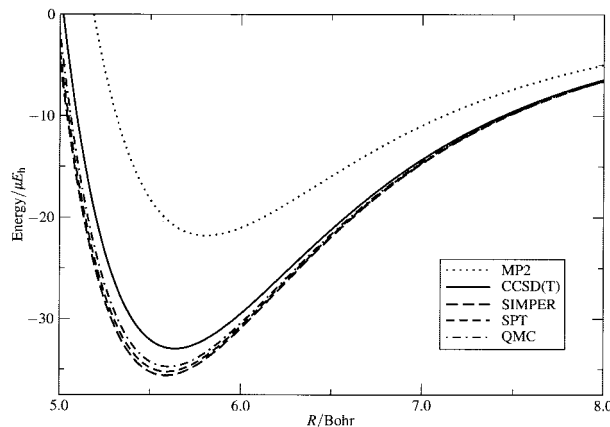


FIGURE 1. Potential energy curves for the $\text{He} \cdots \text{He}$ system calculated using the methods described in the text. The QMC results are taken from Ref. [18].

3. Results

3.1. RARE-GAS DIMERS

3.1.1. Potential Energy Curves

We first compare the potential energy curves for each of the six systems calculated using the SIMPER and SPT methods and the ab initio MP2 and CCSD(T) methods, with the SP-AV5Z basis sets in each case. The MP2/SP-AV5Z results are pertinent because this is the highest level of dimer calculation used by SIMPER and SPT.

Potential energy curves for the six dimers are shown in Figures 1–6, with the methods above plotted against the best available reference data for each system. For the homonuclear systems, these reference data are quantum Monte Carlo (QMC) results for $\text{He} \cdots \text{He}$ [18], estimates of FCI results at the complete basis set (CBS) limit for $\text{Ne} \cdots \text{Ne}$ [19], and the semiempirical HFDID1 [20] potential of Aziz for $\text{Ar} \cdots \text{Ar}$. For $\text{He} \cdots \text{Ne}$ and $\text{He} \cdots \text{Ar}$, we use the HFD-B potentials of Keil et al. [21], and the reported estimated errors in the well depths of 3% are shown in Figures 4 and 5. Finally, for $\text{Ne} \cdots \text{Ar}$ we use the HFD-B* potential determined by Grabow et al. [22]. Values for the binding energies, D_e , and equilibrium separations, R_e , for the six systems are collected in Table I.

Not surprisingly, the MP2 results are poor. Typically, the MP2 dispersion energy coefficients, i.e., those at the UCHF monomer level of theory, significantly underestimate the true values, and this is

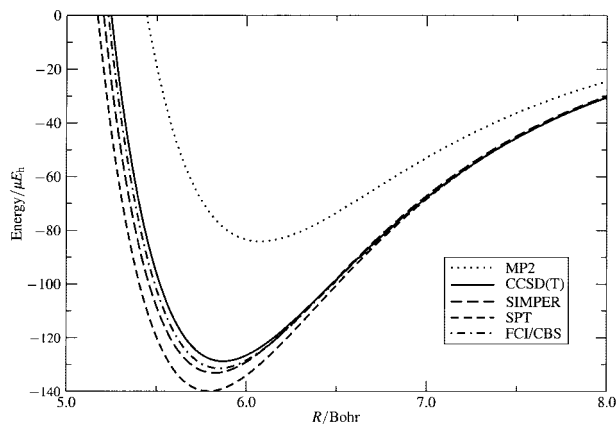


FIGURE 2. Potential energy curves for the Ne \cdots Ne system calculated using the methods described in the text. The FCI/CBS results are taken from Ref. [19].

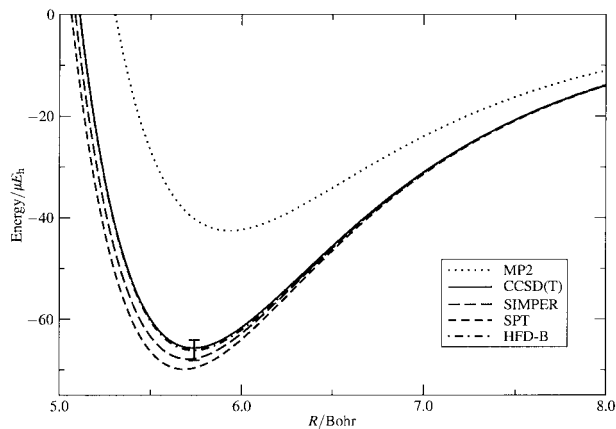


FIGURE 4. Potential energy curves for the He \cdots Ne system calculated using the methods described in the text. The HFD-B results are taken from Ref. [21].

reflected in binding energies that are too small. The argon dimer is the exception to this general trend; the UCHF value for C_6 is too large by nearly 20% and consequently the binding energy is overestimated. The CCSD(T) level of theory provides much more accurate results than MP2, and the binding energies are always too small for these systems. The CCSD(T)/SP-AV5Z errors are largest for He \cdots He and Ar \cdots Ar (about 5%). Results closer to the CBS limit have been presented by Cybulski and Toczyłowski [2] using an augmented AV5Z basis set (AV5Z+). For these more expensive calculations, the largest errors are reduced to about 3%. The CCSD(T)/AV5Z+ results taken from Ref. [2] are also given in Table I.

The SIMPER method can be seen to perform well. For He \cdots He and Ne \cdots Ne, the SIMPER results lie below the accurate QMC and FCI/CBS results by about 0.8 and 1.7 μE_h , respectively. Using the same basis set, the CCSD(T) binding energies are too small by about 1.8 μE_h for He \cdots He, and 2.7 μE_h for Ne \cdots Ne. For Ar \cdots Ar, the SIMPER and CCSD(T) curves are close over a wide range of R , both methods underestimating the HFDID1 binding energy by about 20 μE_h . For the heteronuclear systems, the SIMPER binding energies are larger than the CCSD(T) values. Comparison with the He \cdots Ne and He \cdots Ar is more difficult because of the significant estimated errors in the HFD-B potentials, but in each case the SIMPER binding energies

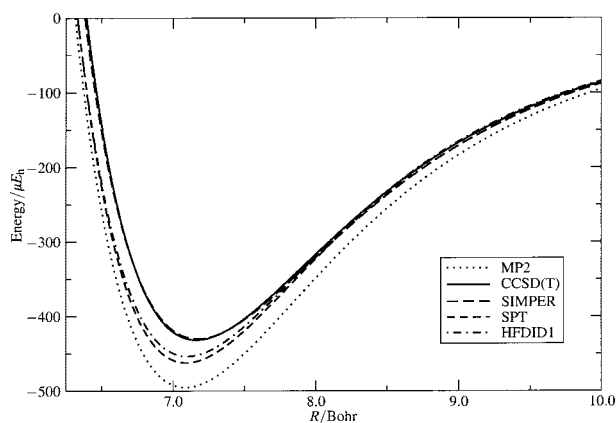


FIGURE 3. Potential energy curves for the Ar \cdots Ar system calculated using the methods described in the text. The HFDID1 results are taken from Ref. [20].

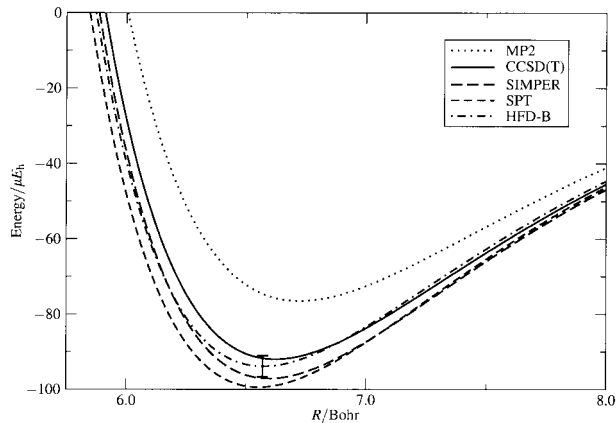


FIGURE 5. Potential energy curves for the He \cdots Ar system calculated using the methods described in the text. The HFD-B results are taken from Ref. [21].

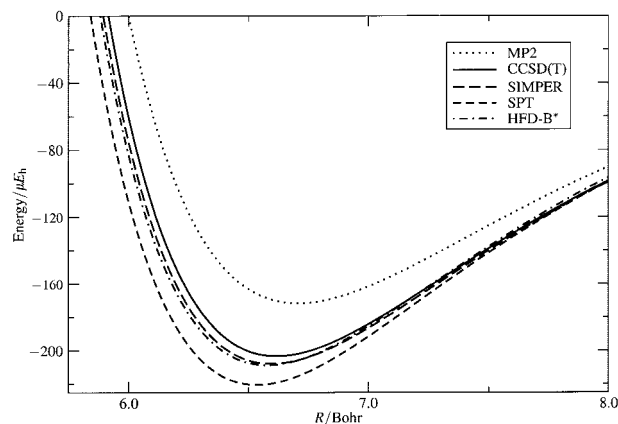


FIGURE 6. Potential energy curves for the Ne \cdots Ar system calculated using the methods described in the text. The HFD-B* results are taken from Ref. [22].

are close to the upper limits. However, for Ne \cdots Ar the SIMPER curve is in good agreement with the HFD-B* results, with the SIMPER binding energy smaller by less than 0.5%.

The improvement in the SIMPER results presented here is a consequence of the better description of the dispersion energy; ab initio dispersion

energy coefficients are used, in conjunction with improved damping functions, as described in Section 2.1. For Ar \cdots Ar the previous results [3] were particularly poor because each C_N was simply scaled by the $C_6^{\text{DOSD}}/C_6^{\text{MP2}}$ ratio, which is $64.30/76.49 \approx 0.84$ for the SP-AV5Z basis set. The MP2 overestimate of C_6 does not apply to the C_8 coefficient, and the isotropic scaling leads to a scaled value of $C_8 = 1281$. The more accurate CISD values calculated here are $C_6 = 66.37$ and $C_8 = 1636$. For systems where the ratio of the C_8 to C_6 values is poor, the damping function scale parameter, b^{MP2} , is also expected to be poor, and these are modified in this work according to Eq. (5). For this improved model, we estimate that the contribution to the dispersion energy from the C_8 term at the minimum is about 25%; C_{10} and C_{12} contribute about 13 and 6%, respectively. For accurate work, the higher dispersion energy coefficients are required, and they contribute around 5% to the dispersion energy for this example. Results based on the scaled RPA values of C_N and the scaling parameters, b^{RPA} , are similar.

In contrast to SIMPER, the SPT method systematically overestimates the binding energies. For He

TABLE I

Binding energies, D_e (μE_h), and equilibrium separations, R_e (Bohr), determined for the potential energy curves calculated in this work [MP2, CCSD(T), SIMPER, and SPT] and reference values from the literature.

Property	MP2	CCSD(T)		SIMPER	SPT	Literature value	Ref.
		SP-AV5Z	AV5Z+				
He \cdots He							
D_e	21.80	32.96	33.67	35.60	35.23	34.77 ± 0.06	[18]
R_e	5.81	5.64	5.62	5.59	5.59	5.60	
Ne \cdots Ne							
D_e	84.07	128.79	130.33	133.13	139.90	131.53 ± 1.1	[19]
R_e	6.08	5.87	5.86	5.82	5.79	5.86	
Ar \cdots Ar							
D_e	495.45	431.61	441.90	430.13	462.24	453.60	[20]
R_e	7.09	7.16	7.14	7.17	7.09	7.10	
He \cdots Ne							
D_e	42.55	65.68	66.57	67.84	69.88	66.15 ± 2	[21]
R_e	5.94	5.74	5.72	5.71	5.68	5.74	
He \cdots Ar							
D_e	76.51	91.99	94.15	97.15	99.43	93.89 ± 3	[21]
R_e	6.72	6.62	6.60	6.60	6.55	6.57	
Ne \cdots Ar							
D_e	171.57	203.24	205.87	207.76	220.44	208.62	[22]
R_e	6.71	6.62	6.60	6.60	6.54	6.58	

The CCSD(T)/AV5Z+ results are taken from Ref. [2].

\cdots He, Ne \cdots Ne, and Ar \cdots Ar, the SPT binding energies are in error by about 1.3, 6.4, and 1.9%, respectively. The corresponding CCSD(T) errors are -5.2 , -2.0 , and -4.8% , so the performance of SPT for He \cdots He and Ar \cdots Ar is better than the CCSD(T) calculations with the same basis sets and worse for Ne \cdots Ne. For He \cdots Ne and He \cdots Ar, we again have to consider the accuracy of the semiempirical HFD-B well depths; in support of this concern is the fact that the CCSD(T)/AV5Z+ calculations have larger binding energies than the HFD-B values [2]. This is in contrast to the homonuclear systems and Ne \cdots Ar. Note that the HFD-B potentials for He \cdots Ne and He \cdots Ar are fitted using experimental differential cross-section and diffusion coefficient data [21], whereas the HFD-B* potential for Ne \cdots Ar is fitted using microwave transitions measured for several isotopomers. The well depth for the HFD-B* potential is therefore likely to be more accurate than those for the two HFD-B models, and the SPT binding energy for Ne \cdots Ar is larger than the HFD-B* value by about 5.7%.

One aspect of previous work using SPT potentials is adjustment to reproduce a single or small number of accurate interaction energies. For Ne \cdots Ne, the SPT interaction energy at $R = 5.84$ Bohr is too negative by about $6 \mu E_h$. The induction and second-order exchange contributions here are small and not likely to account for a large fraction of this error. The dispersion energy contributes a large amount to the interaction energy (about $-263 \mu E_h$), but the model is expected to be accurate; we use values of $C_6 = 6.383$ (the DOSD value) and $C_8 = 84.91$, which compare well with the CISD values of $C_6 = 6.235$ and $C_8 = 84.68$. The SPT and CISD C_8/C_6 ratios are 13.3 and 13.6, respectively, so in addition to the C_N the SPT damping functions are also expected to be accurate [see Eq. (5)]. Note that substituting the CISD values of C_8 and the higher C_N for the scaled RPA values has a negligible effect on the SPT interaction energy. Also to consider are basis set incompleteness, the accuracy of the overlap model that we are using [Eq. (2)], and the quality of the monomer charge densities. We are unable to test at present the effect of missing electron correlation effects in the charge densities, but we note that for the helium dimer, for which all monomer correlation effects are accounted for, we estimated that Eq. (2) is accurate to about 1% [6]. We can reproduce the Gdanitz FCI/CBS estimate of the interaction energy at $R = 5.84$ Bohr by scaling the first-order exchange energies by 1.0489, and the

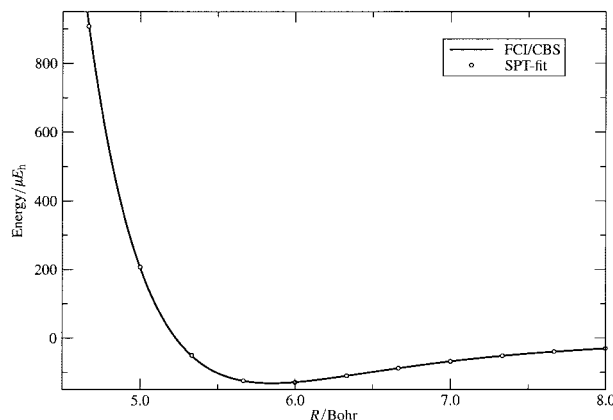


FIGURE 7. Potential energy curves for the Ne \cdots Ne system calculated using the methods described in the text. The FCI/CBS results are taken from Ref. [19].

results for this curve, denoted SPT-fit, are shown alongside the FCI/CBS data in Figure 7. Despite the fact that only the FCI/CBS energy at the minimum is used, the SPT-fit curve is in excellent agreement with the high-quality data both in the repulsive wall and the minimum-energy region, suggesting that this approach has a physically reasonable basis.

3.1.2. Rovibrational Energy Levels

To test the reliability of the calculated potential energy curves, we calculate the energy differences associated with rovibrational transitions. First, we fit the calculated MP2, SIMPER, and SPT energies to the following functional form:

$$V(R) = A \cdot \exp(-bR) - \frac{c}{(R+u)^\delta} - \frac{d}{(R+u)^\delta}, \quad (9)$$

where A , b , c , d , and u are parameters of the fit. To account for the rotational contribution to the energy, we add to $V(R)$ the centrifugal potential

$$V_{\text{rot}}(R) = \hbar^2 J(J+1)/(2\mu R^2), \quad (10)$$

where μ is the reduced mass, and solve the 1-D Schrödinger equation numerically using the Fourier grid Hamiltonian (FGH) method to obtain rovibrational wave functions and energies [23].

The frequencies of the vibrational transitions for Ne \cdots Ar obtained for the SIMPER and SPT curves and those using the HFD-B [24] and HFD-B* potentials [22] are given in Table II. The HFD-B and HFD-B* results have been calculated by us, using

TABLE II
Energy differences (cm^{-1}) between vibrational levels for $\text{Ne} \cdots \text{Ar}$.

$\nu' - \nu''$	MP2	CCSD(T)	SIMPER	SPT	HFD-B	HFD-B*
1 - 0	15.89	18.45	18.56	19.49	19.09	18.78
2 - 1	7.98	9.89	10.22	10.89	10.60	10.19
3 - 2	2.35	3.60	3.70	4.14	3.86	3.54

The MP2, SIMPER, and SPT data are obtained using the SP-AV5Z basis set. The CCSD(T) results, using the AV5Z+ basis set, are taken from Ref. [2].

the FGH method, for consistency with the other results. We also include the results based on the low-level MP2 potentials and the CCSD(T)/AV5Z+ data of Cybulski and Toczyłowski, taken from Ref. [2]. It is evident from Table II that our values of the energy differences between vibrational levels obtained for the extrapolated SIMPER and SPT curves are consistently in good agreement with the best calculated literature CCSD(T) data and also with the results based on the semiempirical HFD-B and HFD-B* potentials. On the other hand, the MP2 results are poor, reflecting the deficiencies in the potential energy curves.

In Table III, we present the energy differences between rotational levels of the ground vibrational state for all three heteronuclear dimers. For $\text{Ne} \cdots \text{Ar}$ we compare the results obtained with the extremely accurate microwave frequency measurements of Grabow et al. [22] for the first three transitions. For the fourth transition, we cite the energy difference calculated by Cybulski and Toczyłowski

[2] using the values of B_0 , D_J , and H_J given by Grabow et al. [22]. For the systems containing He, our results are compared with those calculated by Ogilvie and Wang [25] using a Dunham-type expansion of the potentials. Overall, our results are in good agreement with the literature values. For $\text{Ne} \cdots \text{Ar}$, the SIMPER results underestimate the actual frequencies of rotational transitions but remain within 0.7% of the experimental values. For $\text{He} \cdots \text{Ne}$ and $\text{He} \cdots \text{Ar}$, SIMPER overestimates the semiempirical data of Ogilvie and Wang. The SPT method overestimates the frequencies in all cases.

3.2. $\text{H}_2 \cdots \text{Ne}$ AND $\text{H}_2 \cdots \text{Ar}$ COMPLEXES

The $\text{H}_2 \cdots \text{Ne}$ and $\text{H}_2 \cdots \text{Ar}$ potential energy surfaces can be represented by an expansion in Legendre polynomials:

$$V(R, r, \theta) = \sum_{\lambda} V_{\lambda}(R, r) P_{\lambda}(\cos \theta), \quad (11)$$

TABLE III
Energy differences (cm^{-1}) between rotational levels of the ground vibrational state of an indicated dimer.

$j' - j''$	MP2	CCSD(T)	SIMPER	SPT	Literature value	Ref.
He \cdots Ne						
1 - 0	0.5267	0.7092	0.7179	0.7302	0.7060	[25]
2 - 1		1.3387	1.3592	1.3877	1.3480	[25]
He \cdots Ar						
1 - 0	0.5489	0.5895	0.5941	0.6031	0.5897	[25]
2 - 1	1.0822	1.1671	1.1770	1.1950	1.1670	[25]
3 - 2	1.5789	1.7180	1.7347	1.7622	1.7170	[25]
Ne \cdots Ar						
1 - 0	0.1855	0.1929	0.1931	0.1971	0.1944	[22]
2 - 1	0.3705	0.3856	0.3863	0.3940	0.3887	[22]
3 - 2	0.5553	0.5780	0.5788	0.5906	0.5826	[22]
4 - 3	0.7392	0.7698	0.7706	0.7866	0.7759	[22]

The MP2, SIMPER, and SPT data are obtained using the SP-AV5Z basis set. The CCSD(T) results using the AV5Z+ basis set are taken from Ref. [2].

where R is the distance between the H_2 center of mass and the rare-gas atom, r the H_2 bond length, and θ the angle between the H_2 axis and the line connecting the H_2 center of mass and the rare gas atom. Truncating Eq. (11) at $\lambda = 2$, we need only consider the parallel (linear) and perpendicular (T-shaped) cuts through the potential energy surface because

$$\begin{aligned} V_{\parallel} &= V_0 + V_2, \\ V_{\perp} &= V_0 - V_2/2, \end{aligned} \quad (12)$$

and hence

$$\begin{aligned} V_0 &= (V_{\parallel} + 2V_{\perp})/3 \\ V_2 &= 2(V_{\parallel} - V_{\perp})/3. \end{aligned} \quad (13)$$

For convenience, we drop the dependence on R and r from the notation; in this work we do not consider the dependence of the potential energy surfaces on r , and only consider $r = 1.449$ Bohr (the vibrationally averaged value of r in the ground state). We calculate linear and T-shaped cuts through the $H_2 \cdots Ne$ and $H_2 \cdots Ar$ surfaces using the MP2, CCSD(T), SIMPER (for $H_2 \cdots Ne$ only), and SPT methods. The MP2 and CCSD(T) calculations are performed using AV6Z basis sets.

Results using the above methods are shown for $H_2 \cdots Ne$ in Figure 8, along with the HFD-B results of Rodwell and Scoles [26] (models B and C for the V_0 and V_2 dispersion terms, respectively). The MP2

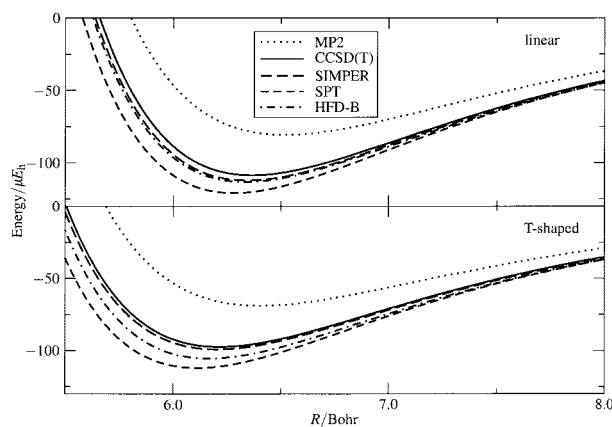


FIGURE 8. Potential energy curves for the $H_2 \cdots Ne$ system, in linear and T-shaped configurations, calculated using the methods described in the text. The HFD-B results are taken from Ref. [26].

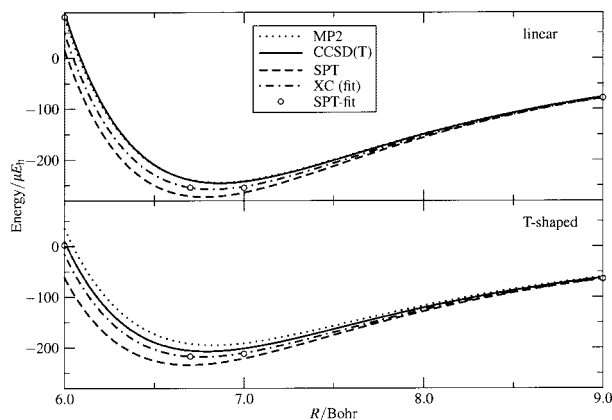


FIGURE 9. Potential energy curves for the $H_2 \cdots Ar$ system, in linear and T-shaped configurations, calculated using the methods described in the text. The XC (fit) results are taken from Ref. [27].

results are significantly shallower than the CCSD(T) results for both orientations, and the SIMPER and CCSD(T) results are in excellent agreement. The SPT method probably overestimates the binding energies, as for the other systems discussed here, so SIMPER and SPT can reasonably be expected to provide lower and upper bounds to the binding energies: 112–121 μE_h for the linear configuration and 98–112 μE_h for the T-shaped configuration.

For $H_2 \cdots Ar$, a number of potentials have been developed but the most accurate is probably the recent XC (fit) potential of Bissonnette et al. [27]. This is based on ab initio calculations, with both short- and long-range parameters adjusted to reproduce spectroscopic and thermodynamic data. The SIMPER method cannot be used for this system because the partitioning of the MP2 interaction energy into Coulomb and exchange contributions [Eq. (3)] is unstable at values of R close to the potential energy minimum. The MP2, CCSD(T), SPT, and XC (fit) results are shown in Figure 9. Interestingly, for the linear configuration the MP2 and CCSD(T) results are similar, although for the T-shaped configuration the CCSD(T) results are somewhat deeper. The SPT curves lie below the XC (fit) data, for which the binding energies should be accurate. We derive SPT-fit models, where we scale the first-order exchange energies by 1.0335 and 1.0491 for the linear and T-shaped geometries, respectively, to reproduce the XC (fit) interaction energies at 6.7 Bohr. These scaling factors are similar to the one used for $Ne \cdots Ne$ (1.0489) and yield potential energy curves in good agreement with the XC (fit) data both in the repulsive wall and the well.

4. Conclusions

We describe two methods, SIMPER and SPT, for calculating intermolecular potentials for weakly bound systems based on low-level supermolecule dimer and perturbation theory calculations. We apply these methods to homonuclear and heteronuclear rare-gas dimers and the $\text{H}_2 \cdots \text{Ne}$ and $\text{H}_2 \cdots \text{Ar}$ complexes. Both methods compare favorably with computationally more expensive dimer calculations; the CCSD(T) method systematically underestimates binding energies for these systems, whereas SPT systematically overestimates them. An improved model for the SIMPER dispersion energy leads to better results than reported previously, especially for $\text{Ar} \cdots \text{Ar}$. A simple scaling procedure yields modified SPT potential energy curves in excellent agreement with existing data for $\text{Ne} \cdots \text{Ne}$ and $\text{H}_2 \cdots \text{Ar}$. The partitioning of the MP2 supermolecule energy into exchange and Coulomb components is found to be unstable for $\text{H}_2 \cdots \text{Ar}$, and work is underway to resolve this problem.

ACKNOWLEDGMENTS

This work was funded by the Engineering and Physical Sciences Research Council. M.P.H. thanks the Leverhulme Trust for financial support.

References

1. Aziz, R. A. In Klein, M. L., Ed. *Inert Gases*; Springer: Berlin, 1984, pp. 5–86. Interatomic potentials for rare-gases: pure and mixed interactions.
2. Cybulski, S. M.; Toczyłowski, R. R. *J Chem Phys* 1999, 111, 10520.
3. Bichoutskaia, E.; Hodges, M. P.; Wheatley, R. J. *J Comput Meth Sci Eng* 2002, 2, 391.
4. Wheatley, R. J.; Price, S. L. *Mol Phys* 1990, 69, 507.
5. Hodges, M. P.; Wheatley, R. J. *Chem Phys Lett* 2000, 326, 263.
6. Hodges, M. P.; Wheatley, R. J. *J Mol Struct Theochem* 2002, 591, 67.
7. Werner, H.-J.; Knowles, P. J.; Amos, R. D.; Berning, A.; Cooper, D. L.; Deegan, M. J. O.; Dobbyn, A. J.; Eckert, F.; Hampel, C.; Hetzer, G.; Leininger, T.; Lindh, R.; Lloyd, A. W.; Meyer, W.; Mura, M. E.; Nicklass, A.; Palmieri, P.; Peterson, K.; Pitzer, R.; Pulay, P.; Rauhut, G.; Schütz, M.; Stoll, H.; Stone, A. J.; Thorsteinsson, T. *MOLPRO*; University of Birmingham: Birmingham, UK, 1997.
8. Boys, S. F.; Bernardi, F. *Mol Phys* 1970, 19, 553.
9. Extensible Computational Chemistry Environment Basis Set Database, version 1/02/02; Molecular Science Computing Facility (MSCF), Environmental and Molecular Sciences Laboratory, Pacific Northwest Laboratory: Richland, WA, 2002.
10. Dunning, T. H. *J Chem Phys* 1989, 90, 1007.
11. Hodges, M. P.; Wheatley, R. J.; Harvey, A. H. *J Chem Phys* 2002, 117, 7169.
12. Tang, K. T.; Toennies, J. P. *J Chem Phys* 1984, 80, 3726.
13. Wheatley, R. J.; Mitchell, J. B. O. *J Comput Chem* 1994, 15, 1187.
14. Hodges, M. P.; Wheatley, R. J. *J Chem Phys* 2001, 114, 8836.
15. Hodges, M. P.; Wheatley, R. J.; Harvey, A. H. *J Chem Phys* 2002, 116, 1397.
16. Margoliash, D. J.; Meath, W. J. *J Chem Phys* 1978, 68, 1426.
17. Kumar, A.; Meath, W. J. *Mol Phys* 1985, 54, 823.
18. Anderson, J. B. *J Chem Phys* 2001, 115, 4546.
19. Gdanitz, R. J. *Chem Phys Lett* 2001, 348, 67.
20. Aziz, R. A. *J Chem Phys* 1993, 99, 4518.
21. Keil, M.; Danielson, L. J.; Dunlop, P. J. *J Chem Phys* 1991, 94, 296.
22. Grabow, J. U.; Pine, A. S.; Fraser, G. T.; Lovas, F. J.; Suenram, R. D.; Emilsson, T.; Arunan, E.; Gutowsky, H. S. *J Chem Phys* 1995, 102, 1181.
23. Marston, C. C.; Balint-Kurti, G. G. *J Chem Phys* 1989, 91, 3571.
24. Barrow, D. A.; Aziz, R. A. *J Chem Phys* 1988, 89, 6189.
25. Ogilvie, J. F.; Wang, F. Y. H. *J Mol Struct* 1993, 291, 313.
26. Rodwell, W. R.; Scoles, G. *J Phys Chem* 1982, 86, 1053.
27. Bissonnette, C.; Chuaqui, C. E.; Crowell, K. G.; Leroy, R. J.; Wheatley, R. J.; Meath, W. J. *J Chem Phys* 1996, 105, 2639.